agronomy

MDPI

Article

The Two Chemotaxis Gene Clusters of *Ensifer alkalisoli* YIC4027^T, a Symbiont of *Sesbania cannabina*, Play Different Roles in Chemotaxis and Competitive Nodulation

Tingting Guo [1,2], Yanan Zhou [1], Zhihong Xie [1,3,*] and Fankai Meng [4]

[1] National Engineering Research Center for Efficient Utilization of Soil and Fertilizer Resources, College of Resources and Environment, Shandong Agricultural University, Taian 271018, China
[2] Department of Molecular Biology, University of Wyoming, Laramie, WY 82071, USA
[3] Key Laboratory of Coastal Environmental Processes and Ecological Remediation, Yantai Institute of Coastal Zone Research, Chinese Academy of Sciences, Yantai 264003, China
[4] Shandong Tunqi Biotechnology Co., Ltd., Jinin 272507, China
* Correspondence: zhxie@yic.ac.cn

Abstract: *Ensifer alkalisoli* YIC4027^T is a dominant rhizobium that has been isolated from the root nodules of *Sesbania cannabina*. Motility and chemotaxis are critical to maintaining competitiveness in establishing the symbiotic relationship. *E. alkalisoli* carries two gene clusters, *che1* and *che2*, containing chemotaxis-related gene homologues. To determine the respective role of each gene cluster, we constructed mutants and compared them with the wild type in a free-living state and in symbiosis with the host plant. A swimming analysis revealed that the *che1* cluster was the major pathway controlling the chemotaxis and swimming bias, while the *che2* cluster had a minor role in these behaviors. However, the Δ*che2* mutant was impaired in exopolysaccharide (EPS) production. During symbiosis, the Δ*che1* mutant was more severely impaired in its competitive root colonization and nodulation ability than the Δ*che2* mutant. Taken together, our data strongly suggested that both of the *che* clusters contribute to the competitive symbiotic association, the *che1*-like homologue being the main regulator of the chemotactic response and the *che2* cluster regulating EPS production. These data illustrated a novel strategy of motile rhizobia bacteria to utilize the two pathways containing the homologous genes to enhance the efficiency of nodule formation by regulating distinct motility parameters or other cellular functions.

Keywords: chemotaxis; *Ensifer alkalisoli*; symbiosis; competitive nodulation

Citation: Guo, T.; Zhou, Y.; Xie, Z.; Meng, F. The Two Chemotaxis Gene Clusters of *Ensifer alkalisoli* YIC4027^T, a Symbiont of *Sesbania cannabina*, Play Different Roles in Chemotaxis and Competitive Nodulation. *Agronomy* **2023**, *13*, 570. https://doi.org/10.3390/agronomy13020570

Academic Editor: José David Flores-Félix

Received: 23 January 2023
Revised: 8 February 2023
Accepted: 8 February 2023
Published: 16 February 2023

1. Introduction

The symbiotic association between rhizobia and legumes is of importance in sustainable agriculture since, within root nodules, rhizobia convert atmospheric dinitrogen (N_2) gas into ammonia, resulting in increased plant growth and productivity [1,2]. The pioneer legume *Sesbania cannabina* is widely cultivated for land reclamation in the area of the Yellow River Delta (Shandong Province in China) due to its outstanding resistance to salt and flooding stress [3,4]. An analysis of the rhizobia from *S. cannabina* root nodules led to the identification of several species of the *Ensifer* genus, which is dominant in the local isolates [5]. Among these, a novel group of *Ensifer* sp. was identified as belonging to a new species, named *Ensifer alkalisoli*, due to its high tolerance to saline–alkaline growth conditions, with YIC4027^T as the type strain [6]. The strain shows high symbiotic efficiency and a narrow host range that is limited to *S. cannabina* [7]. To better understand the molecular basis of its symbiotic association with its host plant, the nucleotide sequence of the complete genome of *E. alkalisoli* YIC4027^T was determined and was fully annotated [7]. Of particular interest were the genes encoding chemotaxis since it is well established that chemotaxis is crucial for nodulation competitiveness in the host plants [8,9].

Chemotaxis, which was studied in detail in *Escherichia coli*, confers in bacteria the ability to move towards attractants or away from repellents [10,11]. The chemotaxis system in *E. coli* contains Che proteins, which are encoded by seven different genes in a single *che* cluster, and chemoreceptors, which are also called methyl-accepting chemotaxis proteins (MCPs) [12]. In brief, chemoreceptors, upon sensing environmental signals, regulate the phosphorylated state of CheA via binding to CheW. Then, the phosphoryl group is transferred from the autophosphorylated CheA to the response regulator CheY. Phospho-CheY then interacts with the flagellar motors to control cell swimming [13,14]. The process is modulated by other Che proteins (CheC, X, D, V, and E) [15–18] in some motile chemotactic bacteria that may carry multiple chemotactic systems [19–21]. The majority of chemosensory pathways control flagellar motility (Fla) [22–24]; however, some are associated with type IV pilus-based motility (TFP) or alternative cellular functions (ACFs) [19,25], such as cell differentiation [26], cell–cell interactions [27,28], and biofilm formation [29–31].

Ensifer alkalisoli YIC4027^T is a motile *Alphaproteobacterium* that contains two chemotaxis (*che*) gene clusters, named *che1* and *che2*, and thirteen putative chemoreceptor genes [7]. The *che1* cluster (EKH55_0219 to EKH55_0228) encodes MCP, CheS, CheY1, CheY2, CheA1, CheW, CheR, CheB, CheD, and CheT and is present on the chromosome [7]. The *che2* cluster (EKH55_5525 to EKH55_5529), which is located on the chromid, contains the genes encoding the CheR, CheW, MCP, CheA2-REC, and CheB proteins [7]. In a previous study, we showed that the gene encoding the histidine kinase in the *che1* cluster, *cheA1*, plays a role in chemotaxis and the symbiotic association between YIC4027^T and *S. cannabina*, while that in cluster *che2*, *cheA2*, was dispensable in this regard [7]. Given the crucial role of the chemotaxis system in bacterial recognition and competitive nodulation [32,33], it is important to determine the respective role of each chemotaxis cluster.

In the present work, we constructed deletion mutant strains covering each *che* gene cluster, *che1* and *che2,* to investigate the contribution of each cluster to the chemotaxis response of *E. alkalisoli* YIC4027^T and to investigate their effect on symbiotic nodulation. Our results showed that the *che1* cluster was essential for chemotaxis motility and that it directly modulated the probability of swimming reversals, providing a competitive advantage for root colonization and nodulation in *E. alkalisoli* YIC4027^T. The *che2* cluster had a minor role in chemotaxis and swimming motility; however, the deletion of the *che2* cluster resulted in impaired EPS production and competitive root colonization and nodulation. Together, these data documented how motile bacteria can utilize two chemotaxis pathways to regulate their chemotactic motility pattern and competitive nodulation.

2. Results

2.1. Comparative Organization of the Chemotaxis Clusters in E. alkalisoli YIC4027^T and Other Alphaproteobacteria

The presence of two chemotaxis gene clusters, named *che1* and *che2*, in the genome of *E. alkalisoli* YIC4027^T was previously reported [7]. Based on the phylogenomic classification [19], *che1* belongs to the F7 system of the Fla class, while *che2* belongs to the ACF class of unknown function. In an attempt to predict the function of the two clusters by comparing them with phylogenetically close microorganisms, we constructed a phylogenetic tree by using the 16S rRNA locus (Figure 1B). From this comparison, it appeared that the *che1* cluster was extremely conserved and that it shared a common gene order with the chemotaxis cluster controlling flagellar motility in *E. meliloti*, *Rhizobium leguminosarum* bv. *viciae*, and *Agrobacterium tumefaciens* [34–36] as well as *Rhizobium etli* [37]. Indeed, the *che1* cluster contained a complete set of genes coding for the chemotaxis proteins known to be in *E. coli* [38], except *cheZ*, and included components that were not seen in *E. coli*, such as the deamidase CheD and the auxiliary protein CheS. The *cheT* gene (orf EKH55_0228), located downstream of *cheD* (Figure 1A,B), was not present in enteric bacteria [8]. Moreover, this set of conserved genes was chromosomally located in all these strains. In addition, the flagellar-motility-related genes (EKH55_0229 to EKH55_0274) (Figure 1A) were located downstream of the *che1* cluster, suggesting that *che1* also controlled flagellar motility. In other strains

which were less phylogenetically close to *E. alkalisoli*, the genes were conserved, but the organization differed.

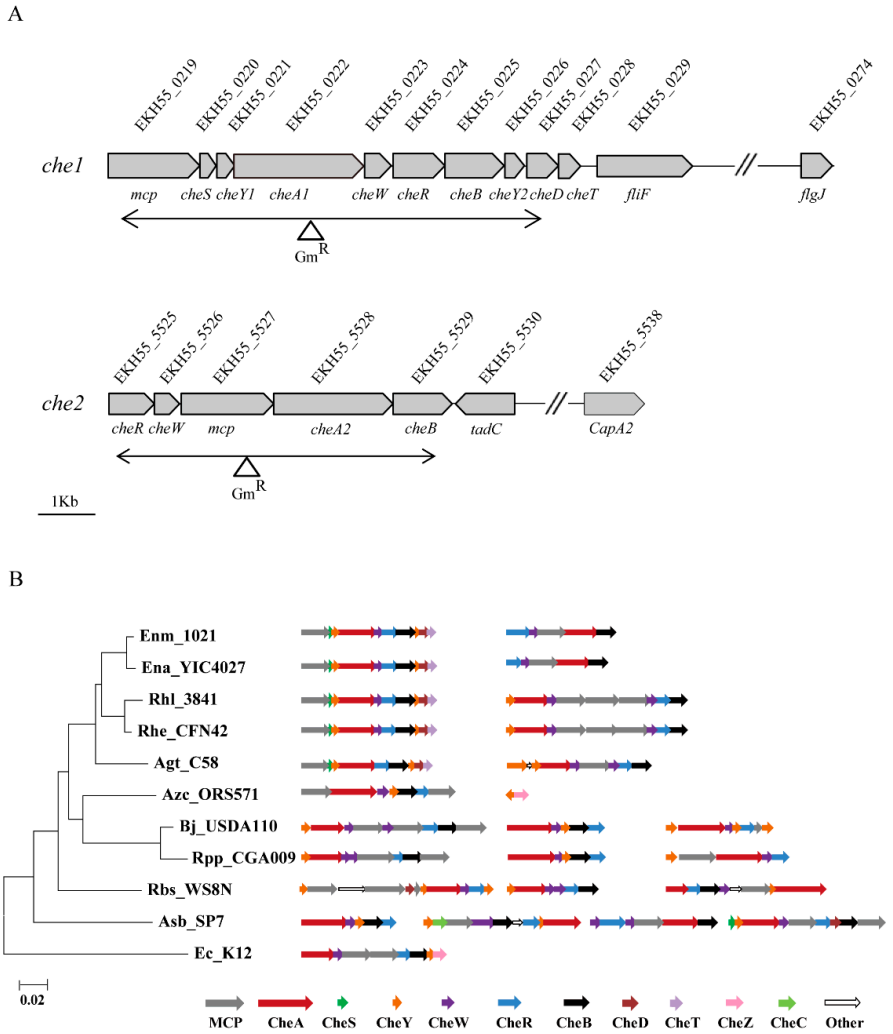

Figure 1. Genetic organization of the chemotaxis gene clusters of *E. alkalisoli* YIC4027^T and comparison with other *Alphaproteobacteria*. (**A**) Genetic organization of the two chemotaxis gene clusters *che1* and *che2* within the *E. alkalisoli* YIC4027^T genome (previously reported in [7]). The double-headed arrow line below each cluster indicates the deleted region in each *che* cluster mutant that yielded Δ*che1* and Δ*che2* mutant strains (see methods). The triangle indicates the insertion of the Gm^R cassette. Gm^R represents gentamicin resistance. Orf represents open reading frame. The open reading frames are drawn to scale. (**B**) Comparison of the chemotaxis gene clusters in the genome of *E. alkalisoli* YIC4027^T and other *Alphaproteobacteria*. Enm represents *Ensifer meliloti*, Ena represents *Ensifer alkalisoli*, Rhl represents *Rhizobium leguminosarum*, Rhe represents *Rhizobium etli*, Agt represents *Agrobacterium tumefaciens*, Azc represents *Azorhizobium caulinodans*, Bj represents *Bradyrhizobium japonicum*, Rpp represents *Rhodopseudomonas palustris*, Rbs represents *Rhodobacter sphaeroides*, Asb represents *Azospirillum brasilense*, and Ec represents *Escherichia coli*. Chemotaxis genes were identified using the MIST3.0 database [39]. The phylogenetic tree was based on 16S rRNA sequences. Strain details are given in Table S1.

The *che2* cluster had a gene order that was identical to that of the corresponding orthologous cluster in phylogenetically closely related *E. meliloti* [8,40]. Although a *che2* orthologue was present in *E. meliloti*, it had weak expression during liquid culture growth, and its function remains to be determined [8,41]. Cluster 2 (EKH55_5525 to EKH55_5529) contained another copy of *mcp*, *cheR*, *cheW*, and *cheB* as well as *cheA2-REC* but did not contain *cheY*, the *cheY2* gene being located in cluster 1. The absence of a *cheY* gene indicated that the *che2* cluster did not control flagella-mediated motility. The genes related to the Flp

pilus assembly (EKH55_5530 to EKH55_5538) were located downstream of the *che2* cluster, suggesting that the *che2* cluster may regulate type IV pilus-mediated motility.

The genes encoding the phosphatases that monitor the dephosphorylation of CheY-P [15], such as the *cheZ* gene, were not present in *Alphaproteobacteria*, except for in *A. caulinodans*, where *cheZ* was adjacent to a *cheY* gene outside of the main chemotaxis cluster [42]. Other genes encoding phosphatases, such as *cheC*, which was found in one of the four clusters of *A. brasilense* [24,43], were not present in *E. alkalisoli*. As phosphorylated CheY1 autodephosphorylates constantly in *E. meliloti*, we can assume that CheY1 might emulate the role of phosphatases in *E. alkalisoli* YIC4027^T. A total of thirteen genes encoding chemoreceptor proteins were annotated in the genome of the YIC4027^T strain, two of them being associated with the *che* clusters [7]. The presence of this large number of chemoreceptor genes suggested that YIC4027^T may sense a variety of chemoattractants or repellents.

2.2. Both the E. alkalisoli YIC4027^T Chemotaxis Clusters were Involved in the Chemotactic Response toward Different Carbon Sources

To characterize the contribution of the *che* clusters to the chemotactic response in YIC4027^T, we constructed strains with in-frame deletions of each *che* cluster from *mcp* to *cheD* for the *che1* cluster and from *cheR* to *cheB* for the *che2* cluster as depicted in Figure 1A. The chemotaxis behavior of the resulting strains, Δ*che1* and Δ*che2*, was compared to that of the wild type and the Δ*cheA1* and Δ*cheA2* mutant strains that were previously constructed [7]. The data were quantified by measuring the chemotaxis diameter rings on soft agar plates containing L3 medium supplemented with various carbon sources. The deletion of the *che1* cluster or the *cheA1* gene resulted in a complete loss of the chemotactic response regardless of the presence or absence of combined nitrogen, while the deletion of the *che2* cluster exhibited an approximately 27% reduction in the chemotaxis ring diameter (Figure 2). However, as reported earlier, the deletion of *cheA2* had no effect on the chemotaxis behavior (Figure 2) [7], suggesting that another gene in the *che2* cluster was involved in the chemotactic response. Both the *che* cluster deletion mutant strains displayed the same growth rate in TY broth medium or L3 minimal medium (Supplementary Figure S1), ruling out that differences in the chemotactic response were related to growth.

A

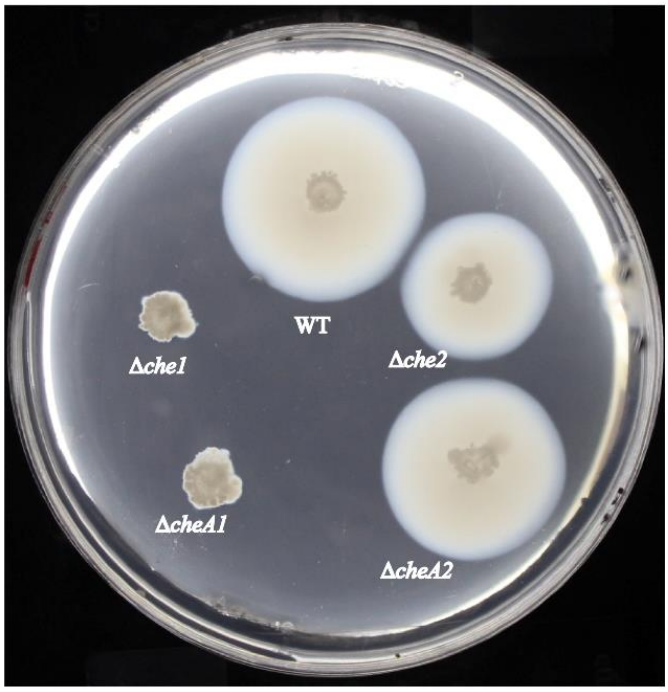

Figure 2. *Cont.*

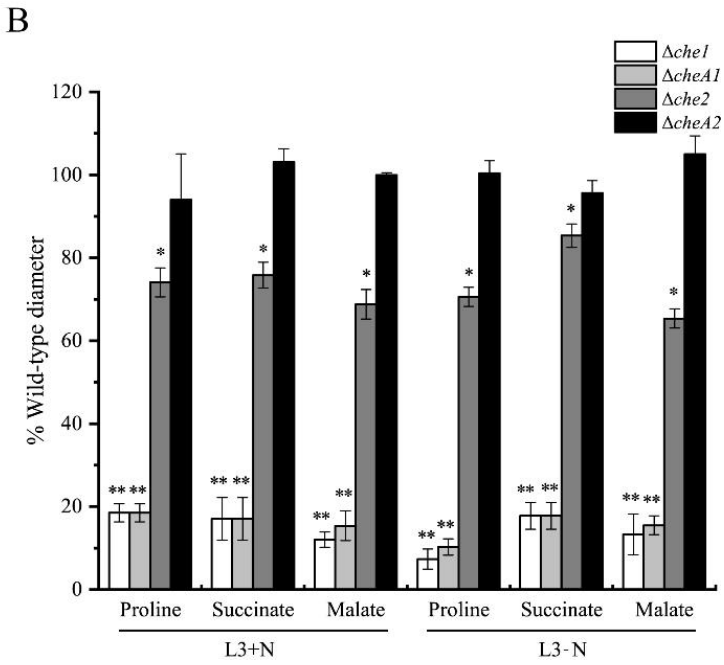

Figure 2. Chemotaxis behavior of *E. alkalisoli* YIC4027^T wild type and deletion mutant strains, Δ*che1*, Δ*che2*, Δ*cheA1*, and Δ*cheA2*, in soft agar plates; WT represents YIC4027^T wild type. (**A**) A representative of L3 plates with proline as the sole carbon source. (**B**) Size of chemotaxis diameter rings produced by wild type and deletion mutants on L3 plates with proline, succinate, or malate as carbon source and with (L3 + N) or without (L3 − N) NH_4Cl as nitrogen source expressed as % of the wild type. Error bars represent standard deviations of the means of three repetitions. * represents $p < 0.05$ versus the WT strain; ** represents $p < 0.01$ versus the WT strain.

2.3. The che1 Cluster was Mainly Involved in the Control of the Swimming Motility Behavior

Chemotaxis ultimately controls the cell swimming motility patterns by affecting the direction of flagellar rotation [10,13,44]. To further investigate the involvement of these two clusters in swimming motility, we compared the swimming behavior of the YIC4027^T wild type and the mutant strains (Figure 3). The wild-type strain showed long runs of swimming interrupted by sudden direction changes (reversals) with an average probability of about 1.14 reversals per second (Supplementary Movie S1). In contrast to the wild type, the Δ*che1* and Δ*cheA1* mutant strains swam in nearly straight lines or constantly ran without reversal (Supplementary Movies S2,3). The Δ*che2* (0.776 reversal/s) mutant displayed a frequency of reversals that was lower than that of the wild-type strain (Supplementary Movie S4). Meanwhile, the reversal frequency of the Δ*cheA2* mutant (1.01 reversals) was similar to that of the wild-type strain (Supplementary Movies S5). These results revealed that the *che1* cluster was essential for changing the swimming direction of the bacterial cells. The lower reversal frequency of the Δ*che2* mutant suggested that the *che2* cluster also played a role in the swimming motility by decreasing the reorientation frequency.

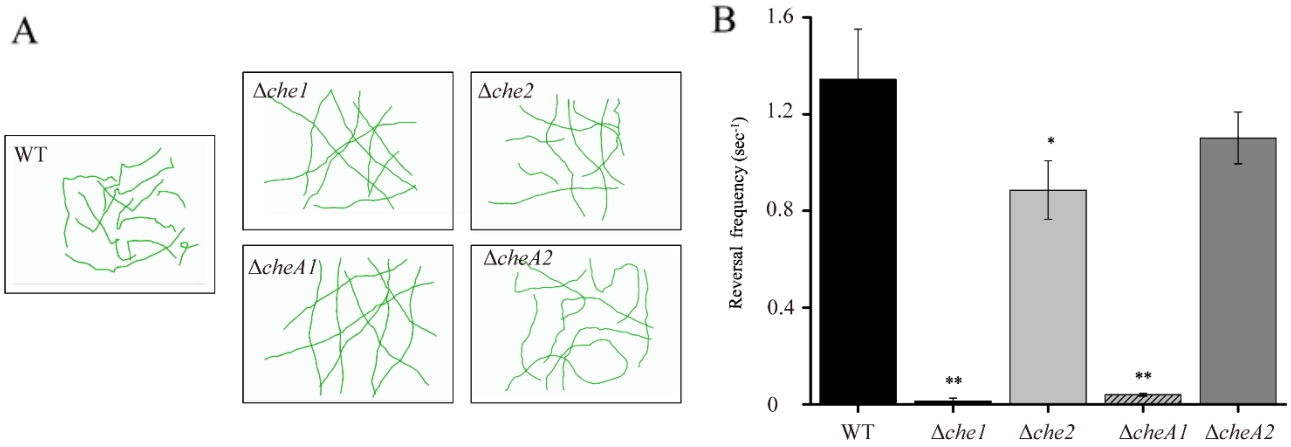

Figure 3. Analysis of swimming behaviors of *E. alkalisoli* YIC4027^T and of Δ*che1*, Δ*che2*, Δ*cheA1*, and Δ*cheA2* mutants. (**A**) Swimming trajectories of *E. alkalisoli* YIC4027^T and its mutants. The tracks were obtained from digital microscope recordings and computerized motion analyses using image processing software (ICY) software (Bioimage Analysis, Paris, France). (**B**) Swimming reversal frequency. Reversals were determined with at least 50 free-swimming cells. Each strain was tested by using at least three independent experiments. Error bars indicate standard deviations of data of the independent experiments. * represents $p < 0.05$ versus the WT strain; ** represents $p < 0.01$ versus the WT strain.

2.4. The che2 Cluster was Involved in EPS Production

The genes controlling chemotaxis and motility in other systems have been reported to affect EPS production [23,30,45,46], an important factor in the establishment of rhizobia–legume symbiosis [47–50]. Thus, the production of EPS by the Δ*che1* and Δ*che2* mutants was further compared with that of the wild type. EPS production by the Δ*che2* mutant was approximately 57% lower than that of the wild type, while no qualitative or quantitative differences were observed between the wild type and the Δ*che1* mutant in EPS production (Figure 4). These data indicated that chemotaxis signaling via *che2* modulated EPS production.

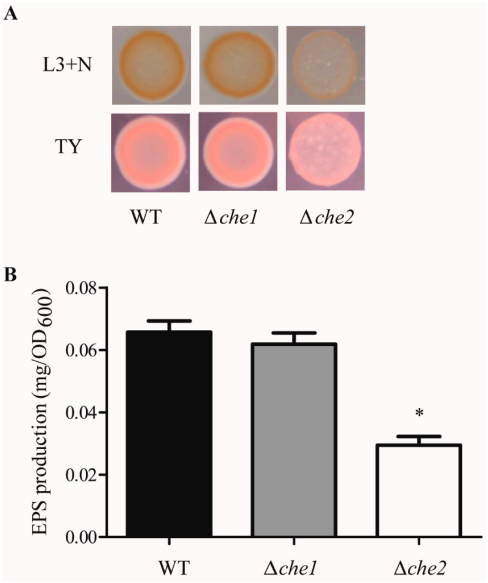

Figure 4. Extracellular polysaccharide (EPS) production of *E. alkalisoli* YIC4027^T wild type and of Δ*che1* and Δ*che2* gene cluster mutants. (**A**) Colonies were grown for 5 days on TY or L3 medium plates containing 0.8% agar and 40 μg/mL of Congo red. **(B)** Quantitative determination of EPS produced by YIC4027^T wild type and *che* mutants. Error bars represent standard deviations of three independent experiments. Asterisks indicate significant differences ($p < 0.05$) between the wild type and the mutants.

2.5. Both the Che Clusters Were Involved in the Competitive Colonization of S. cannabina Roots

Root colonization is the initial step in the establishment of the symbiotic association after initial signaling between plants and rhizobia [51]. Chemotaxis is an important competitive colonization trait, and chemotaxis toward the roots affects rhizobia–legume associations [32,33]. We examined the role of the two chemotaxis gene clusters of *E. alkalisoli* YIC4027^{T} in root colonization. Seedlings that were 2 days old were placed in vermiculite containing a mixture of the wild-type and mutant strains with ratios of 1:1, 1:5, and 1:10 for 5 days. The bacterial strains that were recovered from the inoculated roots were enumerated. As shown in Figure 5, the wild type, when inoculated in numbers equal to each of the mutant strains, performed better than the two chemotaxis cluster mutants, the ratios of the Δ*che1* and Δ*che2* recovered cells being approximately 15% and 39% of that of the wild type, respectively (Figure 5). The number of Δ*che1* and Δ*che2* recovered cells could exceed that of the wild type when the inoculation was performed with a ratio of 1:5 or 1:10 wild type to mutants, the number of the bacteria colonizing the root system being more important in the case of the Δ*che2* mutant than in the case of the Δ*che1* mutant (Figure 5). These results suggested that the Δ*che1* mutant was more severely impaired in its competitive colonization ability than the Δ*che2* mutant.

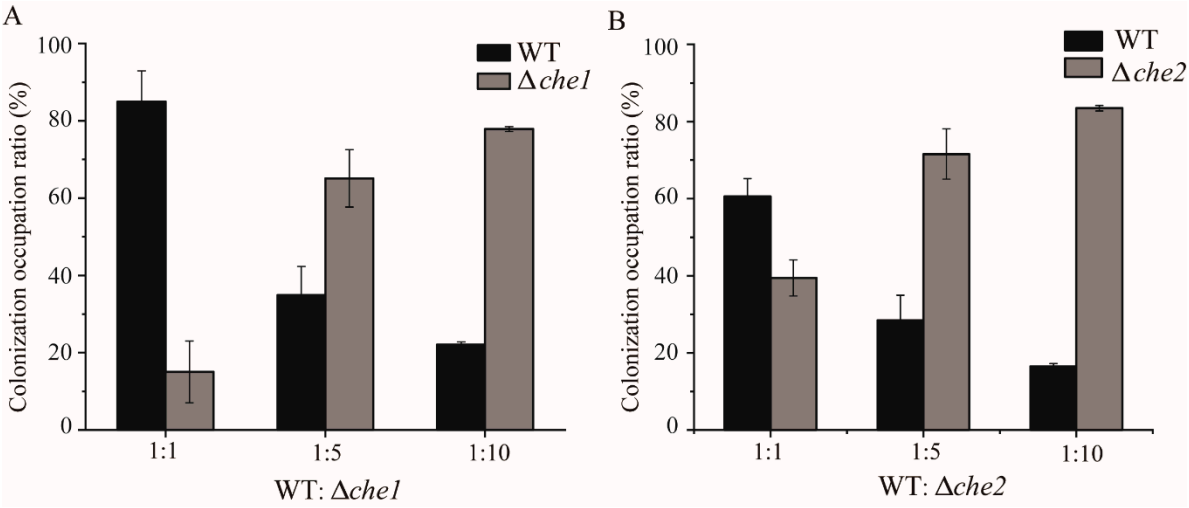

Figure 5. Competitive colonization ability of *E. alkalisoli* YIC4027^{T}WT and mutant strains in the roots of *S. cannabina*. (**A**) Competitive colonization ability of WT and Δ*che1* gene cluster mutant. The x-axis indicates ratios between WT and Δ*che1* mutant. (**B**) Competitive colonization ability of WT and Δ*che2* gene cluster mutant. The x-axis indicates ratios between WT and Δ*che2* mutant. Error bars indicate standard deviations of three independent experiments.

2.6. Both the Che Clusters Modulated Competitive Nodulation

Root colonization is essential for the effective symbiotic nodulation of *S. cannabina* [51]. To further test whether the chemotaxis cluster mutants had any effect on symbiotic nodulation, the nodulation ability was compared between the wild type and the mutants. When inoculated alone in the roots of *S. cannabina*, the Δ*che1* and Δ*che2* mutants formed normal root nodules with no obvious differences between their number and morphology and those of the nodules induced by the wild type (Figure 6A). In addition, inoculated plant growth did not differ (Figure 6B). Furthermore, the competitive nodulation ability in the roots was compared between the wild type and the Δ*che1* and Δ*che2* mutants. Both the mutants were impaired in their ability to compete with the wild type for root nodulation no matter what ratio of bacterial wild-type–mutant strains was used for inoculation (Figure 6C,D).

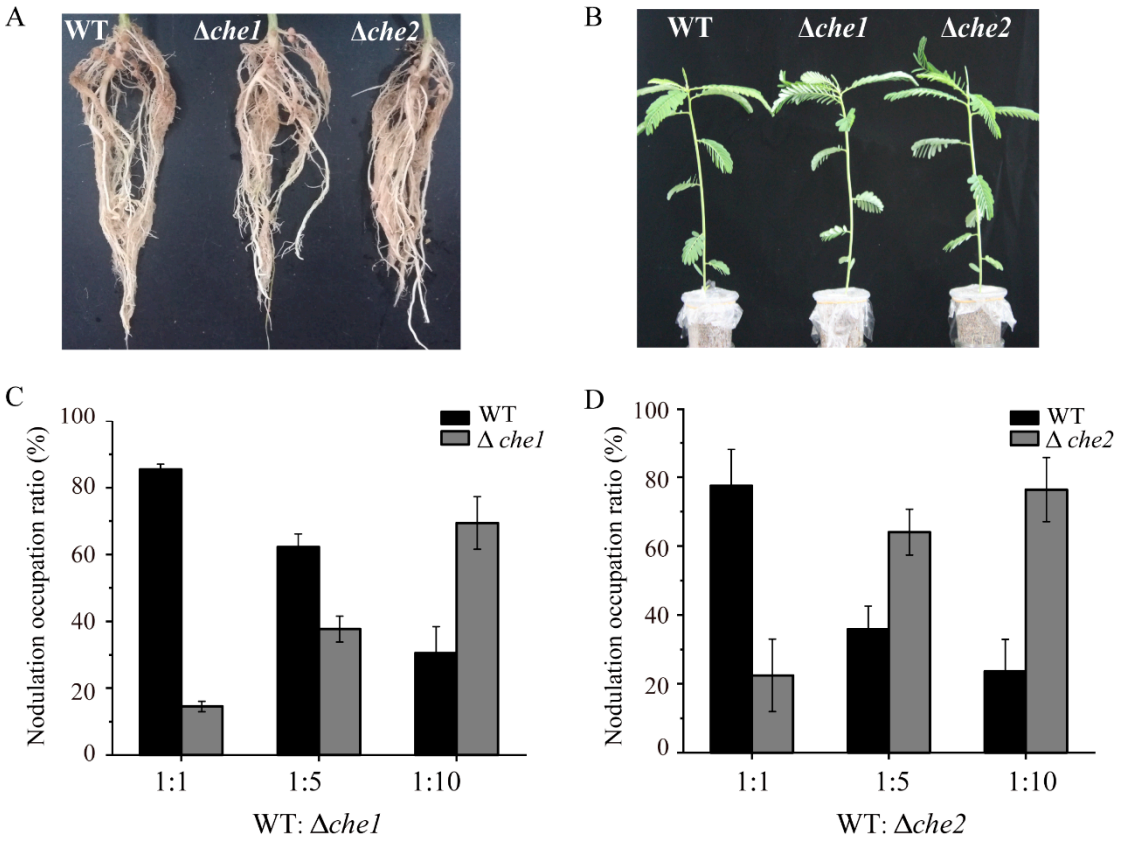

Figure 6. Nodulation assays of *E. alkalisoli* YIC4027^T wild-type and mutant strains in the roots of *S. cannabina*. (**A**) Root nodules induced by WT and Δ*che1* and Δ*che2* mutant strains. (**B**) Representative photographs of the host plant *S. cannabina* inoculated with the wild type or Δ*che1* or Δ*che2* mutants alone. **(C)** Competitive nodulation ability of WT and Δ*che1* mutant. The x-axis indicates ratios between WT and Δ*che1* mutant. (**D**) Competitive nodulation ability of WT and Δ*che2* mutant. The plants were grown at 27 °C for 5 weeks. The x-axis indicates ratios between WT and Δ*che2* mutant. Error bars represent standard deviations of the means of three independent experiments.

3. Discussion

Ensifer alkalisoli YIC4027^T, a dominant species in the saline–alkaline soils of the Yellow River Delta, establishes a nitrogen-fixing symbiosis within the roots of *S. cannabina* and possesses a high degree of nodulation competitiveness [5]. The two chemotaxis systems of YIC4027^T may account for its high nodulation competitivity compared to that of the other rhizobia present in the same soil. In general, the chemotaxis pathways found in bacterial genomes have been found to regulate flagellar motility [22,24] as established, for example, in *E. coli* [52,53] or *A. caulinodans* ORS571 [23]. Many species of *Alphaproteobacteria*, however, carry more than one *che* cluster; *Rhodobacter sphaeroides*, for instance, carries three clusters containing chemotaxis genes, two of which can control the ability to stop flagellar rotation [54]. In *E. alkalisoli* YIC4027^T, both the chemotaxis signaling pathways function in chemotaxis and the regulation of swimming reversal. The contribution of Che1 and Che2 to these behaviors are, however, significantly different: the *che1* cluster is essential for chemotaxis responses and swimming reversal due to a lack of nontumbling ability, while the *che2* cluster has a minor role in chemotaxis and swimming reversal. Interestingly, the *che1* cluster of *E. meliloti*, which is very similar to that of *E. alkalisoli*, also controls chemotaxis and the swimming speed [34,55]. The role of the *che2* cluster in this species remains, as of now, unknown. Since both the species are phylogenetically close, one could assume that the *E. meliloti che2* cluster could have a role similar to that found in YIC4027^T.

In particular, in this work, we reported a link between EPS synthesis and the chemotaxis cluster *che2*. The chemotaxis pathways have been implicated in EPS biosynthesis in other organisms, such as *A. caulinodans* ORS571 [23,41,45], *A. brasilense* [23,27], *Myxococcus xanthus* [56,57], and *Nostoc punctiforme* [58]. In *A. caulinodans* ORS571, several *che* genes were also shown to be involved in EPS production through an unknown mechanism [23,41,45]. In *A. brasilense*, a chemotaxis-like pathway of the ACF class was predicted to regulate EPS production [27]. In *Myxococcus xanthus*, the interactions between Dif and the Che7 pathway have been implicated in EPS production [56,57]. In *Nostoc punctiforme*, a chemotaxis-like gene cluster named *hmp* regulates EPS production by regulating the transcription of the *hsp* genes [58]. The data reported here also suggested that the *che2* cluster in YIC4027^T plays a role in the total amount of EPS produced as observed after the Congo red staining of the colonies and after quantitative determination. Further studies are needed to determine the mechanism underlying the link between chemotaxis and motility in the regulation of EPS biosynthesis. The synthesis of EPS as well as cyclic glucan has been extensively studied in *E. meliloti*, and a complex regulation circuitry involving quorum sensing has been shown [59,60]. So far, the involvement of the *che2* cluster in EPS synthesis has not been shown in *E. meliloti*. It is possible that the two species have similar regulatory circuits that share common genetic determinants; however, this remains to be elucidated.

Chemotaxis and motility are important for the ability to colonize roots (e.g., in *Azospirillum* [24]) and, therefore, also for the symbiotic association of rhizobia with their host plant. According to the classification, the *che1* cluster of *E. alkalisoli* YIC4027^T is a representative of the F7 class (Fla group) of the chemotaxis system, which was shown to be more important in rhizospheric bacteria than in those occurring in bulk soils [19,61]. This chemotaxis system is thought to provide the bacterial strains with a competitive advantage in this environment [24]. In contrast, the *che2* cluster of the YIC4027^T strain belongs to the ACF evolutionary class [19]. The results suggested that this system has a newly discovered function in controlling EPS production and that it is important for competitive nodulation, thus indicating that this pathway also contributes to the rhizosphere lifestyle of this bacterial strain.

In conclusion, we demonstrated that the two chemotaxis clusters in *E. alkalisoli* YIC4027^T have distinct roles. The *che1* cluster is required for chemotaxis motility and competitive nodulation, while the *che2* cluster provides a competitive advantage in root nodulation through the regulation of EPS biosynthesis. Finally, the role of *che2* in chemotaxis and EPS production expands the range of cellular functions modulated by the chemosensory pathways.

4. Materials and Methods

4.1. Phylogenetic Analysis and Chemotaxis Cluster Comparative Analysis

The phylogenetic tree based on 16S rRNA locus was constructed with the neighbor-joining method using MEGA version 6.0 [62] with 1000 bootstrap replicates. The chemotaxis gene clusters in the bacterial genome were searched for in the Microbial Signal Transduction Database 3.0 (MIST3.0) (https://mistdb.com), which is allowed to access since November 2019 [39].

4.2. Bacterial Strains, Plasmids, and Culture Conditions

The bacterial strains and plasmids used in this study are listed in Table 1. *Ensifer alkalisoli* YIC4027^T wild-type strain and its derivative strains were grown at 30 °C with shaking (180 rpm) in TY medium (5 g/L of tryptone, 3 g/L of yeast extract, and 0.83 g/L of $CaCl_2{\cdot}2H_2O$) or in L3 minimal medium (10 mM KH_2PO_4, 100 µg/mL of $MgSO_4{\cdot}7H_2O$, 40 µg/mL of $CaCl_2{\cdot}2H_2O$, 5.4 µg/mL of $FeCl_3{\cdot}6H_2O$, 50 µg/mL of NaCl, 5 µg/mL of $Na_2MoO_4{\cdot}2H_2O$, 2 µg/mL of biotin, 4 µg/mL of nicotinic acid, and 4 µg/mL of pantothenic acid) supplemented with 10 mM carbon source [63]. When appropriate, 25 µg/mL of nalidixic acid was added to the medium. *Escherichia coli* was grown in LB medium at

37 °C with the following concentrations of antibiotics as required: 50 μg/mL of kanamycin, 50 μg/mL of gentamycin, and 10 μg/mL of tetracycline.

Table 1. Bacterial strains and plasmids used in this study.

Strain or Plasmid	Relevant Properties	Source or Reference
Strains		
E. coli		
DH5α	F– *supE44*, *lacA-U169*, Ψ*80 lacZ*, Δ*M15*, *hsdR17*, *recA1*, *endA1*, *gyrA96*, *thi-1 relA1*	Transgen
Ensifer alkalisoli		
YIC 4027^T	Wild-type strain, Nal^r	Li et al. [6]
Δ*che1*	*E. alkalisoli* YIC 4027^T derivative carrying a deletion in the *che1* gene cluster from *mcp* to *cheD*, Nal^r, Gm^r	This study (see Figure 1)
Δ*che2*	*E. alkalisoli* YIC 4027^T derivative carrying a deletion in the *che2* gene cluster from *cheR* to *cheB*, Nal^r, Gm^r	This study (see Figure 1)
Δ*cheA1*	*E. alkalisoli* YIC 4027^T derivative carrying a deletion of *cheA1*, which encodes histidine kinase CheA1; Nal^r; Gm^r	Dang et al. [7]
Δ*cheA2*	*E. alkalisoli* YIC 4027^T derivative carrying a deletion of *cheA2*, which encodes histidine kinase CheA2; Nal^r; Gm^r	Dang et al. [7]
Plasmids		
pCM351	Mobilizable allelic exchange vector, Gm^r, Tc^r	Marx and Lidstrom [64]
pRK2013	Helper plasmid, ColE1 replicon, Tra$^+$, Km^r	Figurski and Helinski [65]

Nal^r represents nalidixic acid resistance, Gm^r represents gentamicin resistance, Tc^r represents tetracycline resistance, and Km^r represents kanamycin resistance.

4.3. Plasmid and Strain Construction

To construct a *che1* cluster mutant, a 6595 bp DNA region from *mcp* to *cheD* was deleted from the genome of *E. alkalisoli* YIC4027^T and was replaced with a gentamycin marker. This was achieved as follows: an 815 bp fragment upstream of *che1*, including 146 bp of the *mcp* gene, was amplified through PCR using the primer pair Che1UF and Che1UR (Table 2), and an 824 bp downstream fragment, including 222 bp of the *cheD*, was amplified through PCR using the primer pair Che1DF and Che1DR. The PCR product corresponding to the upstream DNA fragment was digested with KpnI-NdeI and then was cloned into plasmid pCM351 [64] to yield pCM351::UF. The PCR product corresponding to the downstream fragment was digested with ApaI-AgeI and was cloned into pCM351::UF. The resulting plasmid, pCM351::UF::DF, was used to transform *E. coli* DH5α, and the construction was checked through DNA sequencing. The recombinant plasmid was transferred into *E. alkalisoli* YIC4027^T with the helper plasmid pRK2013 [65]. A deletion mutant resulting from double homologous recombination was obtained by screening the recombinants for gentamicin resistance and tetracycline sensitivity.

Table 2. Primers used in this study.

Primer	Sequence (5′-3′) *	Purpose
Che1UF-KpnI	GGGGTACCGGTTGAGCGGTGAAGTGAA	Δ*che1* construction
Che1UR-NdeI	GGAATTCCATATGAACGCAAGCTCGATACGC	Δ*che1* construction
Che1DF-ApaI	GGGGGCCCGCTACGGCGTGCATCTGA	Δ*che1* construction
Che1DR-AgeI	CGAGCTCGTGCGGCGGTATGAATGA	Δ*che1* construction
Che2UF-KpnI	GGGGTACCGTGACATTCTGACCGCTTTGG	Δ*che2* construction
Che2UR-NdeI	GGAATTCCATATGGGAAGAAGTGCGTTTCCCGTA	Δ*che2* construction
Che2DF-AgeI	GACCGGTCGAGGCCATAGGCGAGAAG	Δ*che2* construction
Che2DR-SacI	CGAGCTCCAGGAACAAGACAGCCAAACG	Δche2 construction
CheA1-F	GTCAGCGGCACCACCAGAGT	Validation of *che1* and *che2*
CheA1-R	CCAACAGGCTTGAACCCACA	Validation of *che1* and *che2*
CheA2-F	GCGTCGGTACAGGAGATTGTG	Validation of *che1* and *che2*
CheA2-R	GCGAGGAGTTGCGTGAGGAT	Validation of *che1* and *che2*

* Engineered restriction sites are underlined.

To construct a *che2* gene cluster deletion mutant, a 3086 bp DNA region from *cheR* to *cheB* was deleted. To obtain such a mutant, an 810 bp upstream fragment, including 175 bp of *cheR*, was amplified through PCR from the genomic DNA of YIC4027^T using the primer pair Che2UF and Che2UR, and a 686 bp downstream fragment, including 58 bp of *cheB*, was amplified through PCR using the primer pair Che2DF and Che2DR. The upstream fragment was digested with KpnI-NdeI and then was inserted into pCM351 to yield pCM351::UF2. The downstream fragment was digested with AgeI-SacI and then was cloned into pCM351::UF2. The plasmid pCM351::UF::DF2 was transferred into *E. alkalisoli* YIC4027^T through triparental conjugation using pRK2013 as helper plasmid. Correct recombination was verified by screening for gentamicin resistance and tetracycline sensitivity as stated above.

4.4. Soft Agar Chemotaxis Assay

For the soft agar assay, YIC4027^T wild type and Δ*che1*, Δ*che2*, Δ*cheA1*, and Δ*cheA2* mutants were grown overnight in TY medium and then were washed three times with chemotaxis buffer (10 mM K_2HPO_4, 10 mM KH_2PO_4, and 0.1 mM EDTA [pH 7.0]) [66]. The cultures were then adjusted to an optical density of 1.0 at 600 nm (OD_{600}). Thereafter, 5 μL aliquots of cell suspensions were stabbed into the L3 soft agar plates (0.3% agar) containing various 10 mM carbon sources, such as proline, succinate, and malate, with or without NH_4Cl as a nitrogen source. Photographs were taken after 5 days of incubation at 30 °C. The diameter of the chemotaxis ring formed by each tested strain was measured. Experiments were performed three times, with three replicates per sample.

4.5. Growth Curve Assays

To compare the growth of YIC4027^T wild type and Δ*che1* and Δ*che2* mutants, cell density was measured as previously described [7,67] with the following modifications: Cells were cultured overnight in TY medium at 30 °C with shaking (180 rpm). The cultures were washed three times with PBS buffer. Then, cells were inoculated in 50 mL of TY medium or in L3 medium containing 10 mM carbon sources and 10 mM NH_4Cl and were adjusted to an OD_{600} of 0.02. Cultures were grown at 30 °C with shaking (180 rpm), and cell density at OD_{600} was monitored every 2 h. The experiment was carried out three times, with three replicates per sample.

4.6. Analysis of Swimming Behavior

Swimming behavior assay was performed as described in [68]. To test motility, YIC4027^T wild type and Δ*che1*, Δ*che2*, Δ*cheA1*, and Δ*cheA2* mutants were grown in rhizobium basal (RB) medium (3.9 mM KH_2PO_4, 6.1 mM K_2HPO_4, 1 mM $(NH_4)_2SO_4$, 1 mM $MgSO_4$, 0.1 mM NaCl, 0.1 mM $CaCl_2$, 0.001 mM $FeSO_4$, 0.01 mM Na_2MoO_4, 20 μg/L biotin, and 100 μg/L thiamine) with 0.2% mannitol as the sole carbon source [68]. After that, cells were resuspended in RB medium containing 10 mM proline as a chemotactic stimulant [7,68]. A total of 5 microliters of the suspension was introduced to a microscope slide, and the swimming behavior was recorded using an Olympus DP73 digital microscope camera on an Olympus BX53 system microscope at ×40 and ×100 magnifications. The swimming paths of each strain were manually tracked on video recordings by using ICY software [69]. Videos were analyzed to observe the cell paths for 3–4 s. The reorientation frequency was determined by counting the number of changes in swimming direction within 5 s per cell. The reorientation frequencies of at least 50 cells were measured in each experiment. For each strain, at least 3 independent experiments were performed.

4.7. Exopolysaccharide Production

For the examination of EPS production, YIC4027^T wild type and Δ*che1* and Δ*che2* mutant strains were grown overnight and were adjusted to an OD600 of 1.0. Then 10 μL of bacterial suspension was dropped onto plates and incubated at 30 °C for 5 days. Qualitative production of EPS was examined on L3 or TY 0.8% agar plates containing Congo red

(40 μg/mL) as described previously [64]. Quantification of EPS production was performed with the anthrone method according to Nakajima et al. [64] using modifications described in [64]. EPS concentration was determined at OD_{620} by referencing a D-glucose standard curve.

4.8. Root Colonization Assay

Sesbania cannabina seeds were surface sterilized with concentrated sulfuric acid for 30 min and then washed 5 times with sterile water. The seeds were germinated through incubation in the dark on inverted water–agar plates for 2 days at 30 °C. Two germinated seedlings were planted in vermiculite growth chamber and were moisturized with Fahraeus mineral solution (0.1 g/L of $CaCl_2$; 0.12 g/L of $MgSO_4 \cdot 7H_2O$; 0.15 g/L of $Na_2HPO_4 \cdot 2H_2O$; 0.1 g/L of KH_2PO_4; 5 mg/L of Fe-citrate; and 0.07 mg/L each of $CuSO_4 \cdot 5H_2O$, $MnCl_2 \cdot 4H_2O$, $ZnCl_2$, H_3BO_3, and $Na_2MoO_4 \cdot 2H_2O$) [70]. *Ensifer alkalisoli* YIC4027^T wild type and Δ*che1* and Δ*che2* mutants grown in TY medium were transferred to RB medium to find mid-log exponential phase and to ensure motility. Then, the cells were washed and suspended at OD_{600} = 0.4 in Fahraeus medium. YIC4027^T wild type was mixed with Δ*che1* or Δ*che2* mutant strain, respectively, at ratios of 1:1, 1:5, and 1:10. Two microliters of the bacterial mixtures were then inoculated in the center of the vermiculite growth chamber. Each of the 6 treatments was applied to 5 chambers, and the assay was repeated 3 times. The roots were harvested after 5 days, and serial dilutions of the homogenized root samples were plated in TY medium containing nalidixic acid. After 2 days of growth at 30 °C, colonies were further identified through PCR using the primer pairs CheA1-F and CheA1-R or CheA2-F and CheA2-R (Table 2). For each competition experiment, at least 100 colonies were verified through PCR.

4.9. Nodulation and Competitive Nodulation Assays

Nodulation and competitive nodulation assays were carried out as previously described [71] with the following modifications: *Ensifer alkalisoli* YIC4027^T wild type and Δ*che1* and Δ*che2* mutant strains were grown in RB medium to find mid-log phase. Afterwards, centrifugation cells were washed 3 times with Fahraeus mineral solution at an OD_{600} of 0.4. YIC4027^T wild type was mixed with Δ*che1* or Δ*che2* mutant, respectively, in 1:1, 1:5, and 1:10 ratios. The mixture and each strain alone were inoculated with germinated seedlings of *S. cannabina* planted as described above. Each treatment was applied to 10 chambers and was repeated at least 3 times. Plants were grown at 27 °C in the greenhouse with a daylight illumination period of 12 h for 5 weeks and were watered with sterile distilled water every 5 to 7 days. Nodules were harvested, surface sterilized with H_2O_2 (20%) for 10 min, and rinsed with sterilized water 5 times [71]. Then, the nodules were crushed and were plated in TY agar plates supplemented with nalidixic acid. Finally, the colonies were verified by PCR through the use of primer pairs CheA1-F and CheA1-R or CheA2-F and CheA2-R (Table 2).

4.10. Statistical Analysis

To compare the YIC4027^T wild type and mutant phenotypes (chemotaxis, swimming behavior, and EPS quantitation assay), statistical analysis was performed via a one-way analysis of variance by using Statistical Package for the Social Sciences (SPSS) 17.0 software package (IBM, New York, USA). A Student's *t*-test assuming equal variances was used to calculate the *p* values of two means. p values < 0.05 were considered to be significant differences. Each experiment was repeated at least three times.

Supplementary Materials: The following supporting information can be downloaded at https://www.mdpi.com/article/10.3390/agronomy13020570/s1: Movie S1: Swimming paths of YIC4027^T wild-type strain. The cells are hyperactive with long runs alternating with sudden changes in swimming direction. Movie S2: Swimming paths of Δ*che1* mutant cells. The cells are swimming in straight lines without direction changes. Movie S3: Swimming paths of Δ*cheA1* mutant cells. Nearly all cells are swimming in straight lines without direction changes. Movie S4: Swimming paths of Δ*che2* mutant cells. The cells are hyperactive with long runs alternating with sudden direction changes. Movie S5: Swimming paths of Δ*cheA2* mutant cells. The cells are hyperactive with long runs alternating with sudden direction changes. Figure S1. Growth curves of YIC4027^T wild type and Δ*che1* and Δ*che2* mutant strains in TY medium (A) or L3 minimal medium containing 10 mM proline and 10 mM NH_4Cl (B). OD_{600} was measured every two hours. Error bars represent standard deviations of the means of three repetitions.

Author Contributions: Conceptualization, T.G., Y.Z. and Z.X.; methodology, T.G. and Y.Z.; formal analysis, T.G.; data curation, Y.Z. and Z.X.; writing—original draft preparation, T.G.; writing—review and editing, T.G., Y.Z., F.M. and Z.X.; funding acquisition, Z.X. and Y.Z. All authors have read and agreed to the published version of the manuscript.

Funding: This research was funded by the National Key Research and Development Program of China (2022YFD1201700), National Natural Science Foundation of China (32270065), and the Shandong Key Research and Development Program (2021CXGC010804).

Data Availability Statement: The data are contained within the article.

Acknowledgments: We thank Claudine Elmerich for help in improving the manuscript.

Conflicts of Interest: The authors declare no conflict of interest.

References

1. Dwivedi, S.L.; Sahrawat, K.L.; Upadhyaya, H.D.; Mengoni, A.; Galardin, M.; Bazzicalupo, M.; Biondi, E.G.; Hungria, M.; Kaschuk, G.; Blair, M.W.; et al. Advances in host plant and *Rhizobium* genomics to enhance symbiotic nitrogen fixation in grain legumes. *Adv. Agron.* **2015**, *129*, 1–116.
2. Udvardi, M.; Poole, P.S. Transport and metabolism in legume-Rhizobia symbioses. *Ann. Rev. Plant Biol.* **2013**, *64*, 781–805. [CrossRef] [PubMed]
3. Ye, Z.H.; Yang, Z.Y.; Chan, G.Y.S.; Wong, M.H. Growth response of *Sesbania rostrata* and *S. cannabina* to sludge-amended lead/zinc mine tailings: A greenhouse study. *Environ. Int.* **2001**, *26*, 449–455. [CrossRef] [PubMed]
4. Allen, O.N.; Allen, E.K. *The Leguminosae, a Source Book of Characteristics, Uses and Nodulation*; The University of Wisconsin Press: Madison, WI, USA, 1981; Volume 8, p. 12.
5. Li, Y.; Li, X.; Liu, Y.; Wang, E.; Ren, C.; Liu, W.; Xu, H.; Wu, H.; Jiang, N.; Li, Y.; et al. Genetic diversity and community structure of rhizobia nodulating *Sesbania cannabina* in saline-alkaline soils. *Syst. Appl. Microbiol.* **2016**, *39*, 195–202. [CrossRef]
6. Li, Y.; Yan, J.; Yu, B.; Wang, E.; Li, X.; Yan, H.; Liu, W.; Xie, Z. *Ensifer alkalisoli* sp. nov. isolated from root nodules of *Sesbania cannabina* grown in saline-alkaline soils. *Int. J. Syst. Evol. Microbiol.* **2016**, *66*, 5294–5300. [CrossRef] [PubMed]
7. Dang, X.; Xie, Z.; Liu, W.; Sun, Y.; Liu, X.; Zhu, Y.; Staehelin, C. The genome of *Ensifer alkalisoli* YIC4027 provides insights for host specificity and environmental adaptations. *BMC Genom.* **2019**, *20*, 643. [CrossRef]
8. Scharf, B.E.; Hynes, M.F.; Alexandre, G.M. Chemotaxis signaling systems in model beneficial plant-bacteria associations. *Plant Mol. Biol.* **2016**, *90*, 549–559. [CrossRef]
9. Feng, H.; Zhang, N.; Du, W.; Zhang, H.; Liu, Y.; Fu, R.; Shao, J.; Zhang, G.; Shen, Q.; Zhang, R. Identification of chemotaxis compounds in root exudates and their sensing chemoreceptors in plant-growth-promoting rhizobacteria *Bacillus amyloliquefaciens* SQR9. *Mol. Plant Microbe Interact.* **2018**, *31*, 995–1005. [CrossRef]
10. Wadhams, G.H.; Armitage, J.P. Making sense of it all: Bacterial chemotaxis. *Nat. Rev. Mol. Cell Biol.* **2004**, *5*, 1024–1037. [CrossRef] [PubMed]
11. Parkinson, J.S.; Kofoid, E.C. Communication modules in bacterial signaling proteins. *Ann. Rev. Gen.* **1992**, *26*, 71–112. [CrossRef]
12. Hazelbauer, G.L.; Falke, J.J.; Parkinson, J.S. Bacterial chemoreceptors: High-performance signaling in networked arrays. *Trends Biochem. Sci.* **2008**, *33*, 9–19. [CrossRef] [PubMed]
13. Sourjik, V.; Wingreen, N.S. Responding to chemical gradients: Bacterial chemotaxis. *Curr. Opin. Cell Biol.* **2012**, *24*, 262–268. [CrossRef] [PubMed]
14. Stock, J.; Da, R.S. Signal transduction: Response regulators on and off. *Curr. Biol.* **2000**, *10*, R420–R424. [CrossRef] [PubMed]
15. Karatan, E.; Saulmon, M.M.; Bunn, N.W.; Ordal, G.W. Phosphorylation of the response regulator CheV is required for adaptation to attractants during *Bacillus subtilis* chemotaxis. *J. Biol. Chem.* **2001**, *276*, 43618–43626. [CrossRef] [PubMed]
16. Szurmant, H.; Muff, T.J.; Ordal, G.W. *Bacillus subtilis* CheC and FliY are members of a novel class of CheY-P-hydrolyzing proteins in the chemotactic signal transduction cascade. *J. Biol. Chem.* **2004**, *279*, 21787–21792. [CrossRef]

17. Rosario, M.M.L.; Ordal, G.W. CheC and CheD interact to regulate methylation of *Bacillus subtilis* methyl-accepting chemotaxis proteins. *Mol. Microbiol.* **1996**, *21*, 511–518. [CrossRef]
18. Ortega, D.R.; Kjær, A.; Briegel, A. The chemosensory systems of *Vibrio cholerae*. *Mol. Microbiol.* **2020**, *114*, 367–376. [CrossRef]
19. Wuichet, K.; Zhulin, I.B. Origins and diversification of a complex signal transduction system in Prokaryotes. *Sci. Signal.* **2010**, *3*, Ra50. [CrossRef]
20. Hamer, R.; Chen, P.Y.; Armitage, J.P.; Reinert, G.; Deane, C.M. Deciphering chemotaxis pathways using cross species comparisons. *BMC Syst. Biol.* **2010**, *4*, 3. [CrossRef]
21. Porter, S.L.; Wadhams, G.H.; Armitage, J.P. *Rhodobacter sphaeroides*: Complexity in chemotactic signalling. *Trends Microbiol.* **2008**, *16*, 251–260. [CrossRef]
22. Whitchurch, C.B.; Leech, A.J.; Young, M.D.; Kennedy, D.; Sargent, J.L.; Bertrand, J.J.; Semmler, A.B.; Mellick, A.S.; Martin, P.R.; Alm, R.A.; et al. Characterization of a complex chemosensory signal transduction system which controls twitching motility in *Pseudomonas aeruginosa*. *Mol. Microbiol.* **2004**, *52*, 873–893. [CrossRef] [PubMed]
23. Liu, W.; Sun, Y.; Shen, R.; Dang, X.; Liu, X.; Sui, F.; Li, Y.; Zhang, Z.; Alexandre, G.; Elmerich, C.; et al. A Chemotaxis-Like Pathway of *Azorhizobium caulinodans* controls flagella-driven motility, which regulates biofilm formation, exopolysaccharide biosynthesis, and competitive nodulation. *Mol. Plant Microbe Interact.* **2018**, *31*, 737–749. [CrossRef] [PubMed]
24. Mukherjee, T.; Kumar, D.; Burriss, N.; Xie, Z.; Alexandre, G. *Azospirillum brasilense* chemotaxis depends on two signaling pathways regulating distinct motility parameters. *J. Bacteriol.* **2016**, *198*, 1764–1772. [CrossRef] [PubMed]
25. He, K.; Bauer, C.E. Chemosensory signaling systems that control bacterial survival. *Trends Microbiol.* **2014**, *22*, 389–398. [CrossRef]
26. He, K.; Dragnea, V.; Bauer, C.E. Adenylate charge regulates sensor kinase $CheS_3$ to control cyst formation in *Rhodospirillum centenum*. *mBio* **2015**, *6*, e00546-15. [CrossRef] [PubMed]
27. Bible, A.; Russell, M.H.; Alexandre, G. The *Azospirillum brasilense* Che1 chemotaxis pathway controls swimming velocity, which affects transient cell-to-cell clumping. *J. Bacteriol.* **2012**, *194*, 3343–3355. [CrossRef]
28. Siuti, P.; Green, C.; Edwards, A.N.; Doktycz, M.J.; Alexandre, G. The chemotaxis-like Che1 pathway has an indirect role in adhesive cell properties of *Azospirillum brasilense*. *FEMS Microbiol. Lett.* **2011**, *323*, 105–112. [CrossRef]
29. Wang, Y.H.; Huang, Z.; Liu, S.J. Chemotaxis towards aromatic compounds: Insights from *Comamonas testosteroni*. *Int. J. Mol. Sci.* **2019**, *20*, 2701. [CrossRef]
30. Hickman, J.W.; Tifrea, D.F.; Harwood, C.S. A chemosensory system that regulates biofilm formation through modulation of cyclic diguanylate levels. *Proc. Natl. Acad. Sci. USA* **2005**, *102*, 14422–14427. [CrossRef]
31. Matilla, M.A.; Martín-Mora, D.; Gavira, J.A.; Krell, T. *Pseudomonas aeruginosa* as a model to study chemosensory pathway signaling. *Microbiol. Mol. Biol.* **2021**, *85*, e00151-20. [CrossRef]
32. de Weert, S.; Vermeiren, H.; Mulders, I.H.M.; Kuiper, I.; Hendrickx, N.; Bloemberg, G.V.; Vanderleyden, J.; De Mot, R.; Lugtenberg, B.J.J. Flagella-driven chemotaxis towards exudate components is an important trait for tomato root colonization by *Pseudomonas fluorescens*. *Mol. Plant Microbe Interact.* **2002**, *15*, 1173–1180. [CrossRef]
33. Greer-Phillips, S.E.; Stephens, B.B.; Alexandre, G. An energy taxis transducer promotes root colonization by *Azospirillum brasilense*. *J. Bacteriol.* **2004**, *186*, 6595–6604. [CrossRef]
34. Greck, M.; Platzer, J.; Sourjik, V.; Schmitt, R. Analysis of a chemotaxis operon in *Rhizobium meliloti*. *Mol. Microbiol.* **1995**, *15*, 989–1000. [CrossRef]
35. Miller, L.D.; Yost, C.K.; Hynes, M.F.; Alexandre, G. The major chemotaxis gene cluster of *Rhizobium leguminosarum* bv. viciae is essential for competitive nodulation. *Mol. Microbiol.* **2007**, *63*, 348–362. [CrossRef] [PubMed]
36. Wright, E.L.; Deakin, W.J.; Shaw, C.H. A chemotaxis cluster from *Agrobacterium tumefaciens*. *Gene* **1998**, *220*, 83–89. [CrossRef]
37. González, V.; Santamaría, R.I.; Bustos, P.; Hernández-González, I.; Medrano-Soto, A.; Moreno-Hagelsieb, G.; Janga, S.C.; Ramírez, M.A.; Jiménez-Jacinto, V.; Collado-Vides, J.; et al. The partitioned *Rhizobium etli* genome: Genetic and metabolic redundancy in seven interacting replicons. *Proc. Natl. Acad. Sci. USA* **2006**, *103*, 3834–3839. [CrossRef] [PubMed]
38. Parkinson, J.S.; Hazelbauer, G.L.; Falke, J.J. Signaling and sensory adaptation in *Escherichia coli* chemoreceptors: 2015 update. *Trends Microbiol.* **2015**, *23*, 257–266. [CrossRef] [PubMed]
39. Gumerov, V.M.; Ortega, D.R.; Adebali, O.; Ulrich, L.E.; Zhulin, I.B. MiST 3.0: An updated microbial signal transduction database with an emphasis on chemosensory systems. *Nucleic Acids Res.* **2019**, *48*, D459–D464. [CrossRef]
40. Barnett, M.J.; Fisher, R.F.; Jones, T.; Komp, C.; Abola, A.P.; Barloy-Hubler, F.; Bowser, L.; Capela, D.; Galibert, F.; Gouzy, J.; et al. Nucleotide sequence and predicted functions of the entire *Sinorhizobium meliloti* pSymA megaplasmid. *Proc. Natl. Acad. Sci. USA* **2001**, *98*, 9883–9888. [CrossRef]
41. Meier, V.M.; Scharf, B.E. Cellular localization of predicted transmembrane and soluble chemoreceptors in *Sinorhizobium meliloti*. *J. Bacteriol.* **2009**, *191*, 5724–5733. [CrossRef]
42. Liu, X.; Liu, W.; Sun, Y.; Xia, C.; Elmerich, C.; Xie, Z. A *cheZ*-like gene in *Azorhizobium caulinodans* is a key gene in the control of chemotaxis and colonization of the host plant. *Appl. Environ. Microbiol.* **2018**, *84*, e01827-17. [CrossRef] [PubMed]
43. Bible, A.N.; Stephens, B.B.; Ortega, D.R.; Xie, Z.; Alexandre, G. Function of a chemotaxis-like signal transduction pathway in modulating motility, cell clumping, and cell length in the Alphaproteobacterium *Azospirillum brasilense*. *J. Bacteriol.* **2008**, *190*, 6365–6375. [CrossRef] [PubMed]
44. de Beyer, J.A.; Szöllössi, A.; Byles, E.; Fischer, R.; Armitage, J.P. Mechanism of signalling and adaptation through the *Rhodobacter sphaeroides* cytoplasmic chemoreceptor cluster. *Int. J. Mol. Sci.* **2019**, *20*, 5095. [CrossRef] [PubMed]

45. Liu, W.; Bai, X.; Li, Y.; Min, J.; Kong, Y.; Hu, X. CheY1 and CheY2 of *Azorhizobium caulinodans* ORS571 regulate chemotaxis and competitive colonization with the host plant. *Appl. Environ. Microbiol.* **2020**, *86*, e00599-20. [CrossRef] [PubMed]
46. Merritt, P.M.; Danhorn, T.; Fuqua, C. Motility and chemotaxis in *Agrobacterium tumefaciens* surface attachment and biofilm formation. *J. Bacteriol.* **2007**, *189*, 8005–8014. [CrossRef] [PubMed]
47. Leigh, J.A.; Signer, E.R.; Walker, G.C. Exopolysacchride-deficeint mutants of *Rhizobium meliloti* that form ineffective nodules. *Proc. Natl. Acad. Sci. USA* **1985**, *82*, 6231–6235. [CrossRef]
48. Hotter, G.S.; Scott, D.B. Exopolysacchride mutants of *Rhizobium loti* are fully effective on a determinate nodulating host but are ineffective on an indeterminate nodulating host. *J. Bacteriol.* **1991**, *173*, 851–859. [CrossRef]
49. Geddes, B.A.; Gonzalez, J.E.; Oresnik, I.J. Exopolysaccharide production in response to medium acidification is correlated with an increase in competition for nodule occupancy. *Mol. Plant Microbe Interact.* **2014**, *27*, 1307–1317. [CrossRef]
50. Janczarek, M.; Rachwał, K.; Turska-Szewczuk, A. A mutation in *pssE* affects exopolysaccharide synthesis by *Rhizobium leguminosarum* bv. *trifolii*, its surface properties, and symbiosis with clover. *Plant Soil* **2017**, *417*, 331–347. [CrossRef]
51. Feng, H.; Fu, R.; Hou, X.; Lv, Y.; Zhang, N.; Liu, Y.; Xu, Z.; Miao, Y.; Krell, T.; Shen, Q.; et al. Chemotaxis of beneficial rhizobacteria to root exudates: The first step towards root–microbe rhizosphere interactions. *Int. J. Mol. Sci.* **2021**, *22*, 6655. [CrossRef]
52. Parkinson, J.S. Complementation analysis and deletion mapping of *Escherichia coli* mutants defective in chemotaxis. *J. Bacteriol.* **1978**, *135*, 45–53. [CrossRef] [PubMed]
53. Parkinson, J.S. *cheA, cheB*, and *cheC* genes of *Escherichia coli* and their role in chemotaxis. *J. Bacteriol.* **1976**, *126*, 756–770. [CrossRef]
54. Hamblin, P.A.; Maguire, B.A.; Grishanin, R.N.; Armitage, J.P. Evidence for two chemosensory pathways in *Rhodobacter sphaeroides*. *Mol. Microbiol.* **1997**, *26*, 1083–1096. [CrossRef] [PubMed]
55. Sourjik, V.; Schmitt, R. Different roles of CheY1 and CheY2 in the chemotaxis of *Rhizobium meliloti*. *Mol. Microbiol.* **1996**, *22*, 427–436. [CrossRef] [PubMed]
56. Campodonico, E.M.; Zusman, D.R. Developments in defining *dif*. *J. Bacteriol.* **2010**, *192*, 4264–4266. [CrossRef] [PubMed]
57. Black, W.P.; Xu, Q.; Cadieux, C.L.; Suh, S.J.; Shi, W.; Yang, Z. Isolation and characterization of a suppressor mutation that restores *Myxococcus xanthus* exopolysaccharide production. *Microbiology* **2009**, *155*, 3599–3610. [CrossRef]
58. Risser, D.D.; Chew, W.G.; Meeks, J.C. Genetic characterization of the *hmp* locus, a chemotaxis-like gene cluster that regulates hormogonium development and motility in *Nostoc punctiforme*. *Mol. Microbiol.* **2014**, *92*, 222–233. [CrossRef]
59. Marketon, M.M.; Sarah, A.G.; Anatol, E.; González, J.E. Quorum sensing controls exopolysaccharide production in *Sinorhizobium meliloti*. *J. Bacteriol.* **2003**, *185*, 325–331. [CrossRef]
60. Baena, I.; Pérez-Mendoza, D.; Sauviac, L.; Francesch, K.; Martín, M.; Rivilla, R.; Bonilla, I.; Bruand, C.; Sanjuán, J.; Llore, J. A partner-switching system controls activation of mixed-linkage beta-glucan synthesis by c-di-GMP in *Sinorhizobium meliloti*. *Environ. Microbiol.* **2019**, *21*, 3379–3391. [CrossRef]
61. Buchan, A.; Crombie, B.; Alexandre, G.M. Temporal dynamics and genetic diversity of chemotactic-competent microbial populations in the rhizosphere. *Environ. Microbiol.* **2010**, *12*, 3171–3184. [CrossRef]
62. Tamura, K.; Steche, G.; Peterso, D.; Filipski, A.; Kumar, S. MEGA6: Molecular evolutionary genetics analysis version 6.0. *Mol. Biol. Evol.* **2013**, *30*, 2725–2729. [CrossRef] [PubMed]
63. Nakajima, A.; Aono, T.; Tsukada, S.; Siarot, L.; Ogawa, T.; Oyaizu, H. Lon protease of *Azorhizobium caulinodans* ORS571 is required for suppression of *reb* gene expression. *Appl. Environl. Microbiol.* **2012**, *78*, 6251–6261. [CrossRef] [PubMed]
64. Marx, C.J.; Lidstrom, M.E. Broad-host-range *cre-lox* system for antibiotic marker recycling in Gram-negative bacteria. *BioTechniques* **2002**, *33*, 1062–1067. [CrossRef]
65. Figurski, D.H.; Helinski, D.R. Replication of an origin-containing derivative of plasmid RK2 dependent on a plasmid function provided in trans. *Proc. Natl. Acad. Sci. USA* **1979**, *76*, 1648–1652. [CrossRef] [PubMed]
66. Alexandre, G.; Greer, S.E.; Zhulin, I.B. Energy taxis is the dominant behavior in *Azospirillum brasilense*. *J. Bacteriol.* **2000**, *182*, 6042–6048. [CrossRef]
67. Liu, W.; Yang, J.; Sun, Y.; Liu, X.; Li, Y.; Zhang, Z.; Xie, Z. *Azorhizobium caulinodans* transmembrane chemoreceptor TlpA1 involved in host colonization and nodulation on roots and stems. *Front. Microbiol.* **2017**, *8*, 1327. [CrossRef]
68. Götz, R.; Schmitt, R. *Rhizobium meliloti* swims by unidirectional, intermittent rotation of right-handed flagellar helices. *J. Bacteriol.* **1977**, *169*, 3146–3150. [CrossRef]
69. de Chaumont, F.; Dallongeville, S.; Chenouard, N.; Hervé, N.; Pop, S.; Provoost, T.; Meas-Yedid, V.; Pankajakshan, P.; Lecomte, T.; Montagner, Y.L.; et al. Icy: An open bioimage informatics platform for extended reproducible research. *Nat. Methods* **2012**, *9*, 690–696. [CrossRef]
70. Fahraeus, G. The infection of clover root hairs by nodule bacteria studied by a simple glass slide technique. *J. Gen. Microbiol.* **1957**, *16*, 374–381. [CrossRef]
71. Salas, M.E.; Lozano, M.J.; Lopez, J.E.; Draghi, W.O.; Serrania, J.; Torres, T.G.A.; Albicoro, F.J.; Nilsson, J.F.; Pistorio, M.; Del Papa, M.F.; et al. Specificity traits consistent with legume-rhizobia coevolution displayed by *Ensifer meliloti* rhizosphere colonization. *Environ. Microbiol.* **2017**, *19*, 3423–3438. [CrossRef]